ACS NANO

www.acsnano.org

PERSPECTIVE

Spin Polarization in Transport Studies of Chirality-Induced Spin Selectivity

Tianhan Liu* and Paul S. Weiss*

Cite This: *ACS Nano* 2023, 17, 19502−19507

Read Online

ACCESS | Metrics & More | Article Recommendations

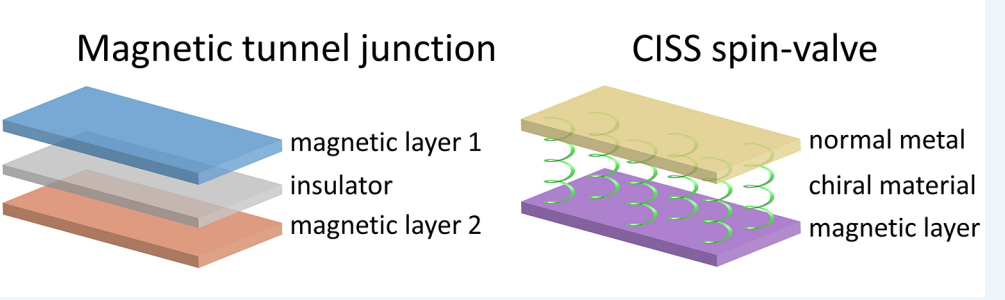

ABSTRACT: **Chirality-induced spin selectivity (CISS) is a recently discovered effect in which structural chirality can result in different conductivities for electrons with opposite spins. In the CISS community, the degree of spin polarization is commonly used to describe the efficiency of the spin filtering/polarizing process, as it represents the fraction of spins aligned along the chiral axis of chiral materials originating from non-spin-polarized currents. However, the methods of defining, calculating, and analyzing spin polarization have been inconsistent across various studies, hindering advances in this field. In this Perspective, we connect the relevant background and the definition of spin polarization, discuss its calculation in different contexts in the CISS, and propose a practical and meaningful figure of merit by quantitative analysis of magnetoresistance in CISS transport studies.**

KEYWORDS: *chirality-induced spin selectivity, spin polarization, transport, spin-valve, magnetic tunnel junction, magnetoresistance*

In chirality-induced spin selectivity (CISS), electron spin can be manipulated without the need for external magnetic fields. In CISS, the conductivity of a charge current passing through chiral media depends on the orientation of electron spins.[1,2] Such an effect has introduced new perspectives to the fields of spintronics and quantum information science.[3−5] One way to quantify the degree of spin alignment in a given direction is through spin polarization (SP). In the context of the CISS, SP describes the spin imbalance from the charge current flowing through a chiral medium. Experimental measurements, theoretical predictions, and calculations have been employed to analyze and to evaluate SP in CISS.[6]

Experimentally, the CISS effect has been predominantly investigated in chiral bioorganic molecules, such as double-stranded DNA and peptides.[1,2] Additionally, other organic and inorganic chiral systems, including chiral hybrid lead iodide perovskites,[7] chiral hybrid copper halides,[8] chiral inorganic oxides,[9] chiral nanofibers,[10,11] chiral metal organic frameworks,[12] and chiral molecular intercalation superlattices,[13] have demonstrated the CISS effect. Three main experimental approaches—photoemission, transport, and chemical reactions—have been employed to study the CISS effect.[6]

In this Perspective, we focus on the definition, calculation, and physical significance of SP in experimental studies of CISS transport, which have not been consistent with its original definition. We identify other relevant physical quantities, such as magnetoresistance, that warrant attention in CISS transport studies beyond the value of SP and propose specific measurement techniques to quantify SP in CISS accurately.

DEFINITIONS OF SPIN POLARIZATION

The most popular and straightforward definition of spin polarization is to use the number of states n or density of states

Received: July 5, 2023
Accepted: September 22, 2023
Published: October 4, 2023

https://doi.org/10.1021/acsnano.3c06133
ACS Nano 2023, 17, 19502−19507

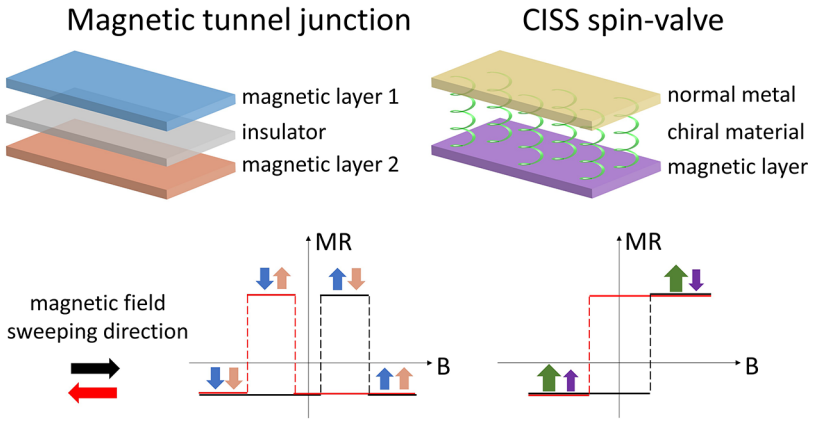

Figure 1. Comparison between a magnetic tunnel junction (MTJ) and a chirality-induced spin selectivity (CISS) spin-valve. Schematics of (top) the structures of (left) a conventional spin-valve and (right) a CISS spin-valve and (below) their corresponding magnetoresistances (MR). The blue, pink, and purple arrows indicate the magnetization directions in the magnetic layers. The green arrow represents the direction of the spin polarization of electrons passing through the chiral media. The MR shows high-resistance states with antiparallel alignment and low-resistance states with parallel alignment. The resistance switches between high and low states in the coercive fields of magnetic layers.

D of spin up ($\uparrow$) and down ($\downarrow$) at the Fermi level. Inside a material, the *intrinsic SP* (SP_i) is:

$$SP_i = \frac{n_\uparrow - n_\downarrow}{n_\uparrow + n_\downarrow} \text{ or } \frac{D_\uparrow - D_\downarrow}{D_\uparrow + D_\downarrow} \quad (1)$$

This relation describes an intrinsic property of a material that does not depend on any measurement.

In various measurements, electrons inside a material can be excited from their ground state by electrons and photons, leading to their subsequent ejection from the material. The SP of electrons is usually considered based on the relative conductance or intensity of the two spin channels. In general, the *measured SP* (SP_m) is:

$$SP_m = \frac{D_\uparrow {\nu_\uparrow}^\alpha - D_\downarrow {\nu_\downarrow}^\alpha}{D_\uparrow {\nu_\uparrow}^\alpha + D_\downarrow {\nu_\downarrow}^\alpha} \quad (2)$$

where ν is the spin-dependent Fermi velocity and α is the weight of the Fermi velocity depending on the experimental setups.[14−16] Specifically, $\alpha = 0$ is for photoemission and tunneling, $\alpha = 1$ is for ballistic transport, and $\alpha = 2$ is for diffusive transport. Therefore, the measured SP_m reflects the intrinsic SP_i of the material only when $\alpha = 0$.

In transport studies, based on Bloch−Boltzmann theory, current density $j \propto D\nu^\alpha$.[14] Equation 2 can be written with $j_{\uparrow(\downarrow)}$, the current density of spin up or down, to quantify the difference in spin-dependent charge currents:[14−16]

$$SP_{tr} = \frac{j_\uparrow - j_\downarrow}{j_\uparrow + j_\downarrow} \quad (3)$$

Here, $j_{\uparrow(\downarrow)}$ are spin-up and down components in the *same* charge current, which are not typically direct observables in experiments. They are usually derived from indirect measurements or from calculations.

CURRENT DEFINITIONS AND ANALYSES OF SPIN POLARIZATION IN CISS TRANSPORT EXPERIMENTS

In CISS transport experiments, one prominent measurement resembles a *spin-valve*, consisting of a normal metal and a magnetic material, with chiral media between the two.[2] This structure can be arranged with a number of approaches, including scanning probe techniques and devices. On one hand, scanning probe methods, such as atomic force microscopy and scanning tunneling microscopy, enable measurements at small scales, ranging from tens of nanometers down to individual molecules.[17] On the other hand, test devices measure the average behavior of chiral media over large scales, typically in the micrometer range, corresponding to the dimensions of the electrodes. Despite different experimental approaches, they all have a spin-valve structure and share the same transport mechanism. When charge current flows through the chiral media, it initiates a spin imbalance that can be detected by the magnetic layer. The magnetization of this layer can often be switched by using an external magnetic field. The device exhibits two resistance states depending on the relative alignment between the magnetization direction in the magnetic layer and the spin polarization from the chiral media.

In recent reports of CISS transport, presumably because $j_{\uparrow(\downarrow)}$ in eq 3 cannot be directly probed in transport measurements, $j_{\uparrow(\downarrow)}$ has been widely replaced by $j_{M\uparrow(\downarrow)}$, the current density with different magnetization directions $M_{\uparrow(\downarrow)}$ in the magnetic layer.[2,7,8,11−13,18−23] The currents with $M_\uparrow$ and $M_\downarrow$ are two *different* currents and *can* be measured directly. Equation 3 has been reported as (with XSP being the incorrectly determined SP):

$$XSP_{CISS} = \frac{j_{M_\uparrow} - j_{M_\downarrow}}{j_{M_\uparrow} + j_{M_\downarrow}} \quad (4)$$

(to the best of our knowledge, the initial definition of XSP can be traced back to the "spin-dependent electrochemistry" section in a review article on CISS[2]).

We note that XSP and SP are two different physical quantities. It will be worth exploring the actual physical significance of XSP. First, we take a closer look at the "spin-valve" structure and how it applies to transport measurements in CISS.

TRADITIONAL SPIN-VALVES: GIANT MAGNETORESISTANCE AND TUNNELING MAGNETORESISTANCE

Traditionally, a spin-valve has a prototypical structure of two magnetic layers separated by and sandwiching a nonmagnetic layer. As the current flows through a spin-valve, its electrical

https://doi.org/10.1021/acsnano.3c06133
ACS Nano 2023, 17, 19502−19507

resistance can change between two values that depend on the relative alignment of the magnetization direction in the two magnetic layers. This effect is called giant magnetoresistance (GMR).[24,25] The main mechanism is spin-dependent scattering based on the relative spin orientations between the electrons and the magnetic layers. As a result, the spin-dependent charge currents with parallel alignment (P) are larger than those with antiparallel alignment (AP). In GMR, the nonmagnetic layer is usually a normal metal with a thickness below the mean free path of the electrons, *i.e.*, typically a few nanometers. Moreover, GMR has been observed not only in magnetic multilayers[24] but also in magnetically inhomogeneous media.[26]

Compared to spin-valves with GMR, the tunneling magnetoresistance (TMR) effect occurs in magnetic tunnel junctions (MTJs) with similar structures and magnetic field dependences.[27−29] MTJs are usually composed of two magnetic layers with an insulating layer in between, as shown in the left panel in Figure 1. In practical traditional spin-valves, the magnetization of one magnetic layer is usually pinned, while the other can be freely rotated; thus, the MR can be continuously changed between two values.

Jullière calculated the relation between the magnetoresistance (MR) and SP in magnetic electrodes as the tunneling conductance being proportional to the product of the spin-related density of states in each electrode, *i.e.*, $D_{1(\uparrow)}D_{2(\uparrow)} + D_{1(\downarrow)}D_{2(\downarrow)}$, where D_1 and D_2 refer to the densities of states in the two electrodes, respectively.[27] The MR in a MTJ can be expressed as:

$$\mathrm{MR_{TMR}} = \frac{G_\mathrm{P} - G_\mathrm{AP}}{G_\mathrm{AP}} = \frac{2(\mathrm{SP_1})(\mathrm{SP_2})}{1 - (\mathrm{SP_1})(\mathrm{SP_2})} \tag{5}$$

where $G_{\mathrm{P(AP)}}$ is the conductance of the TMR structure with parallel (antiparallel) alignment and $\mathrm{SP_1}$ and $\mathrm{SP_2}$ are the intrinsic SPs of the two magnetic layers.

CISS SPIN-VALVES: SIMILARITIES AND DIFFERENCES FROM TRADITIONAL SPIN-VALVES

In a CISS spin-valve, the typical structure is *normal metal layer/chiral material/magnetic layer* (right panel in Figure 1).[2] For simplicity, we present here a device structure with a vertical junction for a CISS spin-valve. Although its fundamental mechanism remains under active investigation,[6] we consider analogies to a MTJ based on their similarities. One can naturally define the MR of a CISS spin-valve as:

$$\mathrm{MR_{CISS}} = \frac{G_\mathrm{P} - G_\mathrm{AP}}{G_\mathrm{AP}} \tag{6}$$

where P (AP) refers to the parallel (antiparallel) alignment between the majority spin orientation of the currents through the chiral media and the magnetization direction of the magnetic layer, assuming positive spin polarization in the magnetic layer.

Other than the similarities, it is important to emphasize the distinctions between a CISS spin-valve and a MTJ.

(1) The SP induced by a charge current through the chiral media primarily relies on the intrinsic properties of the chiral media, such as its handedness and length. It is unaffected by the strength and direction of external magnetic fields. The SP of the chiral layer is usually considered as a constant for a given current along the chiral axis. This situation is different from the manipulation of the magnitude and orientation of the magnetization in a magnetic material.

(2) In a CISS spin-valve, the magnetic layer serves as a spin analyzer to probe the SP from the chiral media, while the normal metal layer primarily functions as an electrode. The chiral media is usually in direct contact with the magnetic layer, *via* monolayer assembly, spin coating, *etc.* In this case, the chiral media serves both as a spacer and as a "spin filter". Although the chiral material itself is not magnetic, the resulting spin-polarized current resembles the itinerant electrons/holes observed in a magnetic material. Poorly conducting organic chiral molecules have often been used as the chiral media. Based on eq 5, one can picture that $\mathrm{SP_1}$ is inherent to the magnetic layer, while the chiral layer produces $\mathrm{SP_2}'$, which is used to distinguish it from $\mathrm{SP_2}$ of the second magnetic layer in a MTJ.

PHYSICAL MEANINGS OF XSP IN CISS SPIN-VALVES

From this basic understanding of a CISS spin-valve and its similarities with and differences from traditional spin-valves (*i.e.*, MTJ), we analyze eq 4 and extract possible physical meanings of XSP. According to the literature on CISS spin-valves, the current−voltage (I−V) curves of such structures are not linear over large current ranges, although various organic and inorganic chiral systems have been studied.[2,7,8,11−13,18−23,30−33] Because of nonlinearities, the conductance $G = \frac{\mathrm{d}j}{\mathrm{d}V}$ is bias dependent. However, in the low-bias regime, comparing the conductance at a fixed current density is common practice in the field of spintronics.[34] Equation 4 can be simplified as:

$$\mathrm{XSP_{CISS}} = \frac{j_{M_\uparrow} - j_{M_\downarrow}}{j_{M_\uparrow} + j_{M_\downarrow}} = \frac{G_\mathrm{P} - G_\mathrm{AP}}{G_\mathrm{P} + G_\mathrm{AP}} \tag{7}$$

Within this approximation, eqs 6 and 7 both depict the conductance asymmetry between different spin states in a spin-valve.[13] From our perspective, XSP solely represents the MR of a CISS spin-valve, offering no additional insight beyond that. However, as elucidated above, it is important to recognize that the physical definitions of MR and SP are distinct.

Moreover, while XSP has been widely interpreted as SP in chiral media, inconsistencies arise when eqs 5 and 7 are combined. For instance, XSP can now be expressed as:

$$\mathrm{XSP_{CISS}} = (\mathrm{SP_1})(\mathrm{SP_2}') \tag{8}$$

In most cases, the magnetic layer is chosen as a conventional ferromagnet, typically with $\mathrm{SP_1} \approx 30\%$. When an unusually large value of XSP is reported, which is significantly larger than the value of $\mathrm{SP_1}$,[7,8,11−13,22,23] it would be required that $\mathrm{SP_2}' = \frac{\mathrm{XSP_{CISS}}}{\mathrm{SP_1}} > 1$. Such values are unphysical, as the value of SP cannot be greater than unity, based on the definitions in eqs 1−3. For example, a spin polarization value (XSP) close to 100% has been reported in a 3D metal−organic framework based on Dy(III) and the L-tartrate chiral ligand by atomic force microscopy with a Co/Cr tip,[12] and two-electrode devices with D/L-alaninol and Al_2O_3 hybrid as the chiral media and Ni as the magnetic layer.[22]

Last but not least, we note that XSP values are shown to depend on the bias in various reports.[8,11,19,22,23] Coverage, packing density, angle relative to the substrate surface, *etc.* can all change the measured values of XSP.[19] The definition of XSP is thus not an intrinsic property, in contrast to the SP in

https://doi.org/10.1021/acsnano.3c06133
ACS Nano 2023, 17, 19502−19507

photoemission and tunneling measurements, which we discuss below.

ANALYZING CISS QUANTITATIVELY AND USING A CONSISTENT FIGURE OF MERIT

Quantitative analyses of (X)SP in CISS transport do not align with the typical definition of SP. Although theoretical calculations can provide estimates,[35] it remains challenging to determine the value of SP in CISS spin-valves experimentally. Instead of focusing on analyzing SP in CISS transport, experimentalists can redirect their attention to measuring MR. The values of MR can be extracted directly as either V/I from the curves of voltage *vs* magnetic field with constant current (or current *vs* magnetic field with constant voltage) or differential conductance, dI/dV, from $I-V$ curves at different fields. Because MR can be obtained directly, it can serve as an important figure of merit from the perspective of applications and is thus an important point of comparison between different molecular systems and test devices.[29] Likewise, theory can be used to understand MR based on the experimental results and can thereby help elucidate the CISS transport process, which remains under debate in various aspects.[6,35−38] Practically, we note a subtle but important point: molecular junctions usually contain parallel conduction, both through molecules and with direct contacts between the top and bottom electrodes, due to pinholes in self-assembled monolayers of molecules.[39] As the conductance in eq 6 often contains the conduction from direct contacts, MR is not an accurate measure to analyze the CISS effect quantitatively. Instead, it would be more rigorous to study ΔG, the conductance difference between the two states of a CISS spin-valve, which depends solely on the CISS effect.[33]

Given the significance of SP in chiral media within the context of CISS, one of the most direct measurements is with photoemission.[40] A Mott polarimeter can be used to measure the imbalance of the light intensities of detectors at opposite channels, to which electrons with spin orientations parallel and antiparallel to their propagation direction are scattered. For example, the SP of ejected photoelectrons from a self-assembled monolayer of double-stranded DNA on a gold substrate was measured and its value exceeded 60% at room temperature.[40] However, photoemission provides the SP of the photocurrent in free space. Furthermore, the measured polarization in photoemission experiments may include the global orbital angular momentum in addition to the SP of photoelectrons.[41] In order to study the SP in a device *via* electrical measurements, one can utilize tunneling junctions consisting of *ferromagnet/insulator/superconductor*.[14,42,43] The technique of spin-polarized tunneling (SPT) has been applied to probe the spin-dependent density of states of magnetic materials by utilizing the special properties of the superconducting states. In practice, one can either fabricate and measure a tunneling junction of *superconductor/chiral material/normal metal* or use spin-polarized scanning tunneling microscopy. In SPT devices, the key is to form a good tunneling barrier so that spin-flip processes such as hopping can be suppressed. For example, a compact and thin insulating layer of Al_2O_3 can be formed from oxidation of the surface layer of the superconducting aluminum electrode of such junctions.[42] In CISS SPT junctions, organic chiral molecules may not be considered as ideal as an insulator because there tends to be pinholes in self-assembled monolayers. One can either assemble chiral materials on an oxide layer to form a *superconductor/oxide/chiral material/normal metal* junction[43] or find insulating chiral solid-state materials to form a junction of *superconductor/insulating chiral solid-state material/normal metal* (see Figure 1 of ref 43 for a schematic of anticipated experimental results).

CONCLUSIONS AND PROSPECTS

The quantitative analysis of (X)SP in CISS transport provides an approximation of the MR in CISS spin-valves, rather than directly indicating the SP of the current passing through chiral media. Therefore, we propose prioritizing the study of the MR in CISS transport. Accurate determination of the SP value can nonetheless be achieved through photoemission measurements or SPT techniques. As the field of CISS remains in the early stages of exploration, it is important to establish consistent and standardized figures of merit for quantification, description, and direct comparisons between systems. Using these figures of merit will facilitate comparisons between experimental findings and theoretical predictions and accelerate our understanding, assessment, and possible application of the CISS effect. In addition, we propose new experimental assemblies to measure SP in transport directly.

AUTHOR INFORMATION

Corresponding Authors

Tianhan Liu − *Department of Chemistry and Biochemistry, University of California, Los Angeles, Los Angeles, California 90095, United States;* orcid.org/0000-0003-3934-0785; Email: tianhanliu@g.ucla.edu

Paul S. Weiss − *Departments of Chemistry and Biochemistry, Bioengineering, and Materials Science and Engineering and California NanoSystems Institute, University of California, Los Angeles, Los Angeles, California 90095, United States;* orcid.org/0000-0001-5527-6248; Email: psw@cnsi.ucla.edu

Complete contact information is available at: https://pubs.acs.org/10.1021/acsnano.3c06133

Notes

The authors declare no competing financial interest.

ACKNOWLEDGMENTS

We are grateful for helpful discussions with Prof. Ron Naaman, Prof. Prineha Narang, Dr. Li Wan, Prof. Peng Xiong, Prof. Binghai Yan, Dr. Qun Yang, Dr. Xiaohang Zhang. T.L. and P.S.W. are supported by National Science Foundation (grant #CHE-2004238) and the W. M. Keck Foundation through the Keck Center on Quantum Biology.

REFERENCES

(1) Naaman, R.; Waldeck, D. H. Chiral-Induced Spin Selectivity Effect. *J. Phys. Chem. Lett.* **2012**, *3*, 2178−2187.

(2) Naaman, R.; Waldeck, D. H. Spintronics and Chirality: Spin Selectivity in Electron Transport through Chiral Molecules. *Annu. Rev. Phys. Chem.* **2015**, *66*, 263−281.

(3) Aiello, C. D.; Abendroth, J. M.; Abbas, M.; Afanasev, A.; Agarwal, S.; Banerjee, A. S.; Beratan, D. N.; Belling, J. N.; Berche, B.; Botana, A.; Caram, J. R.; Celardo, G. L.; Cuniberti, G.; Garcia-Etxarri, A.; Dianat, A.; Diez-Perez, I.; Guo, Y.; Gutierrez, R.; Herrmann, C.; Hihath, J.; et al. A Chirality-Based Quantum Leap. *ACS Nano* **2022**, *16*, 4989−5035.

(4) Chiesa, A.; Privitera, A.; Macaluso, E.; Mannini, M.; Bittl, R.; Naaman, R.; Wasielewski, M. R.; Sessoli, R.; Carretta, S. Chirality Induced Spin Selectivity: An Enabling Technology for Quantum Applications. *Adv. Mater.* **2023**, *35*, 2300472.

(5) National Academies of Sciences, Engineering, and Medicine. *Advancing Chemistry and Quantum Information Science: An Assessment of*

Research Opportunities at the Interface of Chemistry and Quantum Information Science in the United States; The National Academies Press: 2023. DOI: 10.17226/26850
(6) Evers, F.; Aharony, A.; Bar Gill, N.; Entin Wohlman, O.; Hedegård, P.; Hod, O.; Jelinek, P.; Kamieniarz, G.; Lemeshko, M.; Michaeli, K.; Mujica, V.; Naaman, R.; Paltiel, Y.; Refaely Abramson, S.; Tal, O.; Thijssen, J.; Thoss, M.; van Ruitenbeek, J. M.; Venkataraman, L.; Waldeck, D. H.; Yan, B.; Kronik, L. Theory of Chirality Induced Spin Selectivity: Progress and Challenges. *Adv. Mater.* **2022**, *34*, 2106629.
(7) Lu, H.; Wang, J.; Xiao, C.; Pan, X.; Chen, X.; Brunecky, R.; Berry, J. J.; Zhu, K.; Beard, M. C.; Vardeny, Z. V. Spin-Dependent Charge Transport through 2D Chiral Hybrid Lead-Iodide Perovskites. *Sci. Adv.* **2019**, *5*, eaay0571.
(8) Lu, Y.; Wang, Q.; He, R.; Zhou, F.; Yang, X.; Wang, D.; Cao, H.; He, W.; Pan, F.; Yang, Z.; Song, C. Highly Efficient Spin Filtering Transport in Chiral Hybrid Copper Halides. *Angew. Chemie Int. Ed.* **2021**, *60*, 23578−23583.
(9) Ghosh, K. B.; Zhang, W.; Tassinari, F.; Mastai, Y.; Lidor-Shalev, O.; Naaman, R.; Möllers, P.; Nürenberg, D.; Zacharias, H.; Wei, J.; Wierzbinski, E.; Waldeck, D. H. Controlling Chemical Selectivity in Electrocatalysis with Chiral CuO-Coated Electrodes. *J. Phys. Chem. C* **2019**, *123*, 3024−3031.
(10) Jia, L.; Wang, C.; Zhang, Y.; Yang, L.; Yan, Y. Efficient Spin Selectivity in Self-Assembled Superhelical Conducting Polymer Microfibers. *ACS Nano* **2020**, *14*, 6607−6615.
(11) Kulkarni, C.; Mondal, A. K.; Das, T. K.; Grinbom, G.; Tassinari, F.; Mabesoone, M. F. J.; Meijer, E. W.; Naaman, R. Highly Efficient and Tunable Filtering of Electrons' Spin by Supramolecular Chirality of Nanofiber Based Materials. *Adv. Mater.* **2020**, *32*, 1904965.
(12) Huizi-Rayo, U.; Gutierrez, J.; Seco, J. M.; Mujica, V.; Diez-Perez, I.; Ugalde, J. M.; Tercjak, A.; Cepeda, J.; San Sebastian, E. An Ideal Spin Filter: Long-Range, High-Spin Selectivity in Chiral Helicoidal 3-Dimensional Metal Organic Frameworks. *Nano Lett.* **2020**, *20*, 8476−8482.
(13) Qian, Q.; Ren, H.; Zhou, J.; Wan, Z.; Zhou, J.; Yan, X.; Cai, J.; Wang, P.; Li, B.; Sofer, Z.; Li, B.; Duan, X.; Pan, X.; Huang, Y.; Duan, X. Chiral Molecular Intercalation Superlattices. *Nature* **2022**, *606*, 902−908.
(14) Mazin, I. I. How to Define and Calculate the Degree of Spin Polarization in Ferromagnets. *Phys. Rev. Lett.* **1999**, *83*, 1427−1430.
(15) Sanvito, S.; Rocha, A. R. Molecular-Spintronics: The Art of Driving Spin through Molecules. *J. Comput. Theor. Nanosci.* **2006**, *3*, 624−642.
(16) Sanvito, S. Molecular Spintronics. *Chem. Soc. Rev.* **2011**, *40*, 3336.
(17) Donhauser, Z. J.; Mantooth, B. A.; Kelly, K. F.; Bumm, L. A.; Monnell, J. D.; Stapleton, J. J.; Price, D. W., Jr.; Rawlett, A. M.; Allara, D. L.; Tour, J. M.; Weiss, P. S. Conductance Switching in Single Molecules through Conformational Changes. *Science* **2001**, *292*, 2303.
(18) Giaconi, N.; Poggini, L.; Lupi, M.; Briganti, M.; Kumar, A.; Das, T. K.; Sorrentino, A. L.; Viglianisi, C.; Menichetti, S.; Naaman, R.; Sessoli, R.; Mannini, M. Efficient Spin-Selective Electron Transport at Low Voltages of Thia-Bridged Triarylamine Hetero[4]Helicenes Chemisorbed Monolayer. *ACS Nano* **2023**, *17*, 15189−15198.
(19) Clever, C.; Wierzbinski, E.; Bloom, B. P.; Lu, Y.; Grimm, H. M.; Rao, S. R.; Horne, W. S.; Waldeck, D. H. Benchmarking Chiral Induced Spin Selectivity Measurements towards Meaningful Comparisons of Chiral Biomolecule Spin Polarizations. *Isr. J. Chem.* **2022**, *62*, 1−15.
(20) Aragonès, A. C.; Medina, E.; Ferrer-Huerta, M.; Gimeno, N.; Teixidó, M.; Palma, J. L.; Tao, N.; Ugalde, J. M.; Giralt, E.; Díez-Pérez, I.; Mujica, V. Measuring the Spin-Polarization Power of a Single Chiral Molecule. *Small* **2017**, *13*, 1602519.
(21) Mondal, A. K.; Brown, N.; Mishra, S.; Makam, P.; Wing, D.; Gilead, S.; Wiesenfeld, Y.; Leitus, G.; Shimon, L. J. W.; Carmieli, R.; Ehre, D.; Kamieniarz, G.; Fransson, J.; Hod, O.; Kronik, L.; Gazit, E.; Naaman, R. Long-Range Spin-Selective Transport in Chiral Metal-Organic Crystals with Temperature-Activated Magnetization. *ACS Nano* **2020**, *14*, 16624−16633.
(22) Al-Bustami, H.; Khaldi, S.; Shoseyov, O.; Yochelis, S.; Killi, K.; Berg, I.; Gross, E.; Paltiel, Y.; Yerushalmi, R. Atomic and Molecular Layer Deposition of Chiral Thin Films Showing up to 99% Spin Selective Transport. *Nano Lett.* **2022**, *22*, 5022−5028.
(23) Niman, C. M.; Sukenik, N.; Dang, T.; Nwachukwu, J.; Jones, A. K.; Naaman, R.; Santra, K.; Das, T. K.; Paltiel, Y.; Baczewski, L. T.; El-Naggar, M. Y. Bacterial Extracellular Electron Transfer Components are Spin Selective. 2023, chemrxiv-2023−030cv. *ChemRxiv*. DOI: 10.26434/chemrxiv-2023-030cv (Accessed September 12, 2023).
(24) Baibich, M. N.; Broto, J. M.; Fert, A.; Van Dau, F. N.; Petroff, F.; Etienne, P.; Creuzet, G.; Friederich, A.; Chazelas, J. Giant Magnetoresistance of (001)Fe/(001)Cr Magnetic Superlattices. *Phys. Rev. Lett.* **1988**, *61*, 2472−2475.
(25) Parkin, S. S. P. Giant Magnetoresistance in Magnetic Nanostructures. *Annu. Rev. Mater. Sci.* **1995**, *25*, 357−388.
(26) Xiao, J. Q.; Jiang, J. S.; Chien, C. L. Giant Magnetoresistance in Nonmultilayer Magnetic Systems. *Phys. Rev. Lett.* **1992**, *68*, 3749−3752.
(27) Julliere, M. Tunneling between Ferromagnetic Films. *Phys. Lett. A* **1975**, *54*, 225−226.
(28) Moodera, J. S.; Kinder, L. R.; Wong, T. M.; Meservey, R. Large Magnetoresistance at Room Temperature in Ferromagnetic Thin Film Tunnel Junctions. *Phys. Rev. Lett.* **1995**, *74*, 3273−3276.
(29) Yuasa, S. Giant Tunneling Magnetoresistance in MgO-Based Magnetic Tunnel Junctions. *J. Phys. Soc. Jpn.* **2008**, *77*, 031001.
(30) Xie, Z.; Markus, T. Z.; Cohen, S. R.; Vager, Z.; Gutierrez, R.; Naaman, R. Spin Specific Electron Conduction through DNA Oligomers. *Nano Lett.* **2011**, *11*, 4652−4655.
(31) Alam, K. M.; Pramanik, S. Spin Filtering through Single-Wall Carbon Nanotubes Functionalized with Single-Stranded DNA. *Adv. Funct. Mater.* **2015**, *25*, 3210−3218.
(32) Abendroth, J. M.; Cheung, K. M.; Stemer, D. M.; El Hadri, M. S.; Zhao, C.; Fullerton, E. E.; Weiss, P. S. Spin-Dependent Ionization of Chiral Molecular Films. *J. Am. Chem. Soc.* **2019**, *141*, 3863−3874.
(33) Liu, T.; Wang, X.; Wang, H.; Shi, G.; Gao, F.; Feng, H.; Deng, H.; Hu, L.; Lochner, E.; Schlottmann, P.; von Molnár, S.; Li, Y.; Zhao, J.; Xiong, P. Linear and Nonlinear Two-Terminal Spin-Valve Effect from Chirality-Induced Spin Selectivity. *ACS Nano* **2020**, *14*, 15983−15991.
(34) Wang, K.; Sanderink, J. G. M.; Bolhuis, T.; Van Der Wiel, W. G.; De Jong, M. P. Tunnelling Anisotropic Magnetoresistance Due to Antiferromagnetic CoO Tunnel Barriers. *Sci. Rep.* **2015**, *5*, 1−8.
(35) Dalum, S.; Hedegård, P. Theory of Chiral Induced Spin Selectivity. *Nano Lett.* **2019**, *19*, 5253−5259.
(36) Yang, X.; van der Wal, C. H.; van Wees, B. J. Spin-Dependent Electron Transmission Model for Chiral Molecules in Mesoscopic Devices. *Phys. Rev. B* **2019**, *99*, 024418.
(37) Yang, X.; van der Wal, C. H.; van Wees, B. J. Detecting Chirality in Two-Terminal Electronic Nanodevices. *Nano Lett.* **2020**, *20*, 6148−6154.
(38) Xiao, J.; Zhao, Y.; Yan, B. Nonreciprocal Nature and Induced Tunneling Barrier Modulation in Chiral Molecular Devices. *arXiv*. DOI: 10.48550/arXiv.2201.03623 (Accessed September 20, 2023).
(39) Claridge, S. A.; Liao, W. S.; Thomas, J. C.; Zhao, Y. X.; Cao, H. H.; Cheunkar, S.; Serino, A. C.; Andrews, A. M.; Weiss, P. S. From the Bottom Up: Dimensional Control and Characterization in Molecular Monolayers. *Chem. Soc. Rev.* **2013**, *42*, 2725−2745.
(40) Göhler, B.; Hamelbeck, V.; Markus, T. Z.; Kettner, M.; Hanne, G. F.; Vager, Z.; Naaman, R.; Zacharias, H. Spin Selectivity in Electron Transmission through Self-Assembled Monolayers of Double-Stranded DNA. *Science* **2011**, *331*, 894−897.
(41) Liu, Y.; Xiao, J.; Koo, J.; Yan, B. Chirality-Driven Topological Electronic Structure of DNA-Like Materials. *Nat. Mater.* **2021**, *20*, 638−644.
(42) Tedrow, P. M.; Meservey, R. Spin Polarization of Electrons Tunneling from Films of Fe, Co, Ni, and Gd. *Phys. Rev. B* **1973**, *7*, 318−326.

(43) Zhang, X.; McGill, S. A.; Xiong, P.; Wang, X.; Zhao, J. Probing the Thiol-Gold Planar Interface by Spin Polarized Tunneling. *Appl. Phys. Lett.* **2014**, *104*, 152403.

https://doi.org/10.1021/acsnano.3c06133
ACS Nano 2023, 17, 19502−19507